

# Imaging in scattering media via the second-order correlation of light field

Wenlin Gong, Pengli Zhang, Xia Shen, and Shensheng Han\*  
 Key Laboratory for Quantum Optics and Center for Cold Atom Physics of CAS,  
 Shanghai Institute of Optics and Fine Mechanics,  
 Chinese Academy of Sciences, Shanghai 201800, China  
 (Dated: October 25, 2018)

Imaging with the second-order correlation of two light fields is a method to image an object by two-photon interference involving a joint detection of two photons at distant space-time points. We demonstrate for the first time that an image with high quality can still be obtained in the scattering media by applying the second-order correlation of illuminating light field. The scattering effect on the visibility of images is analyzed both theoretically and experimentally. Potential applications and the methods to further improve the visibility of the images in scattering media are also discussed.

PACS numbers: 42.50.Ar, 42.68.Mj, 42.50.Dv, 42.62.Be

Multiple scattering has a great influence on the quality of images. The information will be degraded and the images suffer reduced resolution and contrast because of multiple scattering, such as light propagation and imaging in the atmosphere [1], neutron imaging [2], imaging and diagnosis in life and medical sciences [3]. In medical and clinic diagnosis, comparing with X-ray, optical photons provide nonionizing and safe radiation for medical applications, and are now becoming an increasing interesting method for imaging in biological tissues. Such as Optical coherence tomography (OCT), Diffuse optical tomography (DOT), Photoacoustic tomography (PAT) and so on [4, 5, 6, 7, 8, 9]. Although the quality of images in scattering media have an enhancement in some extent by these techniques, there are still lots of problems which are difficult to be settled. Because all conventional imaging methods are based on first-order correlation of light field, we “see” an image only when we look at the object, which means the detection and imaging are unseparated in conventional imaging process. So when the information of the object is distorted by multiple scattering, and the information of both multiple scattering and the object are unknown, we can not, in principle, obtain exactly an image destroyed by multiple scattering.

With respect to the classical area of imaging, the field of quantum imaging aims to devise novel techniques for optical imaging, by exploiting the quantum nature of light [12]. Based on the characteristic of Bose-Einstein correlation of light fields and the theory of two-photon interference [13], the imaging method by the second-order correlation of two light fields, for example, ghost imaging with entangled source or thermal light, becomes a new kind of imaging technique [14]. In ghost imaging schemes, even if the test detector is a pointlike or bucket detector, by measuring the second-order correlation function of the two light fields, we can still obtain the image of the object with both entangled source and thermal light by scanning the position of the photons which never actually

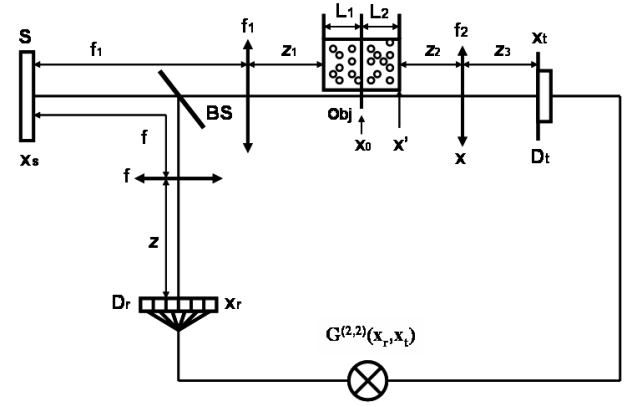


FIG. 1: Scheme for the second-order correlation with thermal light in the scattering media.

passed through the object [15, 16, 17, 18, 19, 20, 21, 22]. This imaging method, for the first time in the history of imaging technology development, leads to the separation of detection and imaging. In this letter, when there is multiple scattering in the test path but no multiple scattering in the reference path, imaging in the scattering media with thermal light is investigated by the second-order correlation of two light fields.

Fig. 1 shows the schematic of experimental setup. The thermal light source  $S$  produced by the method described in Ref. [22, 23, 24], first propagates through a beam splitter, then is divided into a test and a reference path. In the test path, the light goes through a thin lens of focal length  $f_1$ , scattering media and then to the test detector  $D_t$ . In the reference path, the light propagates through another thin lens of focal length  $f$  then to the CCD camera  $D_r$  with the axial resolution  $6.45 \times 6.45 \mu\text{m}$ .

In Fig. 1, The impulse response function between the plane  $x$  and the plane  $x_0$  is [4, 10, 11]

$$h(x, x_0) = \alpha h_{in}(x, x_0) + \beta h_{sca}(x, x_0). \quad (1)$$

$$|\alpha|^2 + |\beta|^2 = 1. \quad (2)$$

\*Electronic address: sshan@mail.shnc.ac.cn

where  $h_{in}(x, x_0)$  is the impulse response function with no scattering media, and  $h_{sca}(x, x_0)$  is the impulse response function because of the interactions of multiple scattering.  $\alpha, \beta$  are the probability amplitudes of incident light and scattering light, respectively.

The probability distribution function in scattering media can be represented by point scattering function (PSF). Generally, there are two forms of PSF: Lorentzian-shaped and Gaussian-shaped distribution [25, 26].

$$h_{sca}(x, x_0) \propto \int dx' P(x', x_0)_{L_A} h(x, x')_{(L_2+z_2)}, \quad (3a)$$

$$P(x', x_0)_{L_A} = \left[ \frac{2}{\pi \Delta x_{L_A}^2} \right]^{1/4} \exp \left\{ -\left( \frac{x' - x_0}{\Delta x_{L_A}} \right)^2 \right\}, \quad (3b)$$

$$\int |P(x', x_0)_{L_A}|^2 dx' = 1. \quad (3c)$$

$$\beta \propto \frac{D^{a_\beta} w^{c_\beta} L_A^{d_\beta} n^{e_\beta}}{\lambda^{b_\beta}}; \Delta x_{L_A} \propto \frac{D^{a_x} w^{c_x} L_A^{d_x} n^{e_x}}{\lambda^{b_x}}. \quad (3d)$$

here,  $P(x', x_0)_{L_A}$  is the Gaussian-shaped point scattering probability amplitude from the position  $x_0$  to  $x'$  when the light goes through the scattering medium with effective thickness  $L_A$ .  $\Delta x_{L_A}$ ,  $D$ ,  $w$ ,  $\lambda$  and  $n$  are the broadening width, the diameter size of scattering particles, the concentration of suspended particles, the wavelength of the incident light and refractive index of the scattering medium, respectively.  $\alpha, \beta$  and  $\Delta x_{L_A}$  are all determined by specific experimental conditions.

By optical coherence theory [13, 17, 18], the second-order correlation function between the two detectors is:

$$\begin{aligned} \Delta G^{(2,2)}(x_r, x_t) &= \langle I(x_r) I(x_t) \rangle - \langle I(x_r) \rangle \langle I(x_t) \rangle \\ &= \left| \int dx_1 \int dx_2 G^{(1,1)}(x_1, x_2) h_r^*(x_1, x_r) h_t(x_2, x_t) \right|^2. \end{aligned} \quad (4)$$

where  $\langle \rangle$  denotes statistical average of the ensemble, and  $G^{(1,1)}(x_1, x_2)$  is the first-order correlation function on the source plane,  $h_t(x_t, x_2)$  is the impulse response function in the test path whereas  $h_r^*(x_r, x_1)$  denotes phase conjugate of the impulse response function in the reference path.

Suppose the light source is fully spatially incoherent,

$$G^{(1,1)}(x_1, x_2) = I_0 \delta(x_1 - x_2). \quad (5)$$

where  $I_0$  is a constant, and  $\delta(x)$  is Dirac delta function.

Under the paraxial approximation, and when the effective apertures of the lenses in the optical system are large enough, the impulse response function of the reference system is

$$h_r(x_r, x_1) \propto \exp \left\{ \frac{j\pi}{\lambda f} \left( 1 - \frac{z}{f} \right) x_1^2 - \frac{2j\pi}{\lambda f} x_r x_1 \right\}. \quad (6)$$

when the object plane, the thin lens  $f_2$  and the test detector plane satisfy the thin lens equation

$$\frac{1}{z_2 + L_2} + \frac{1}{z_3} = \frac{1}{f_2}. \quad (7)$$

then the impulse response function in the test path is

$$\begin{aligned} h_t(x_t, x_2) &\propto \int dx' [\alpha_1 \exp \left\{ -\frac{2j\pi}{\lambda f_1} x' x_2 \right\} + \beta_1 \int dx'_2 \\ &\times P(x', x'_2)_{L_{1A}} \exp \left\{ -\frac{2j\pi}{\lambda f_1} x'_2 x_2 \right\}] t(x') C(x') \\ &\times \exp \left\{ \frac{j\pi}{\lambda f_1} \left( 1 - \frac{z_1 + L_1}{f_1} \right) x_2^2 \right\}. \end{aligned} \quad (8a)$$

$$C(x') = \alpha_2 \delta \left( x' + \frac{z_2 + L_2}{z_3} x_t \right) + \beta_2 P \left( -\frac{z_2 + L_2}{z_3} x_t, x' \right)_{L_{2A}} \quad (8b)$$

where  $t(x)$  is the transmission function of the object. If

$$\frac{1 - \frac{z}{f}}{f} = \frac{1 - \frac{z_1 + L_1}{f_1}}{f_1}. \quad (9)$$

and  $\frac{f_1}{f} = \frac{z_2 + L_2}{z_3}$ , then the same speckle distributions can be obtained on the two detector planes without the scattering media and the object. Substituting Eqs. (5)-(9) into Eq. (4), the correlation function is

$$\begin{aligned} \Delta G^{(2,2)}(x_r, x_t) &\propto \left\{ \alpha_1 \alpha_2 \delta(x_r + x_t) + P \left( -\frac{f_1}{f} x_t, \frac{f_1}{f} x_r \right)_{L_{2A}} \right. \\ &\times \beta_1 \alpha_2 \left. \right\} t \left( -\frac{f_1}{f} x_t \right) + \alpha_1 \beta_2 P \left( -\frac{f_1}{f} x_t, \frac{f_1}{f} x_r \right)_{L_{1A}} t \left( \frac{f_1}{f} x_r \right) \\ &+ \beta_1 \beta_2 \int dx' (x') P \left( x', \frac{f_1}{f} x_r \right)_{L_{1A}} P \left( -\frac{f_1}{f} x_t, x' \right)_{L_{2A}} \left. \right|^2 \end{aligned} \quad (10)$$

If the test detector is a bucket detector, integrating  $x_t$  in Eq. (10), then

$$\Delta G^{(2)}(x_r) = \int \Delta G^{(2,2)}(x_r, x_t) dx_t. \quad (11)$$

If the test detector is a CCD camera, because the images on the two camera planes are inverse, in the case of  $x_t = -x_r$ , Eq. (10) can be rewritten as

$$\begin{aligned} \Delta G^{(2,2)}(x_r, -x_r) &\propto \left\{ \alpha_1 \alpha_2 + \alpha_1 \beta_2 \left[ \frac{2}{\pi \Delta x_{L_{2A}}^2} \right]^{1/4} \right. \\ &+ \beta_1 \alpha_2 \left. \left[ \frac{2}{\pi \Delta x_{L_{1A}}^2} \right]^{1/4} \right\} t \left( \frac{f_1}{f} x_r \right) + \beta_1 \beta_2 C_0 \left. \right|^2. \end{aligned} \quad (12)$$

$$C_0 = \int dx' t(x') P \left( x', \frac{f_1}{f} x_r \right)_{L_{1A}} P \left( \frac{f_1}{f} x_r, x' \right)_{L_{2A}}. \quad (13)$$

From Eq. (12)-(13), for  $L_1=0$  (namely,  $\beta_1=0$ ) or  $L_2=0$  (namely,  $\beta_2=0$ ), images with high quality can always be

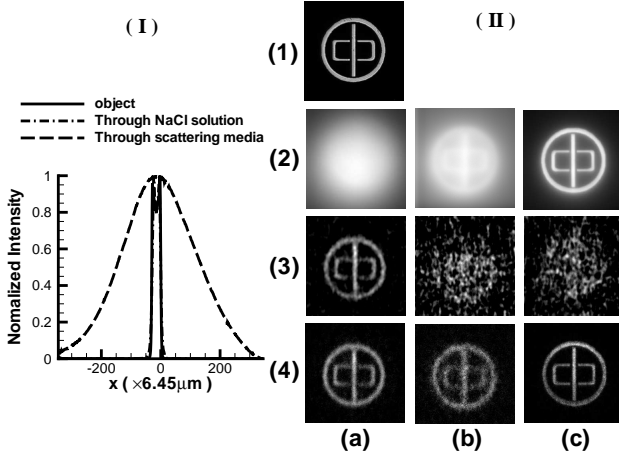


FIG. 2: (I). The axial sections of the images when the thermal light from a single slit (the slit width  $a=0.2\text{mm}$ ) fixed before the mediums went through different mediums with the scattering thickness  $L_1 + L_2=40\text{mm}$ . (II). Images of the object obtained when the sample was fixed in different positions of the scattering media (averaged 15, 000 speckle frames). (a).  $L_1=0\text{mm}, L_2=40\text{mm}, \Delta x_{LA}=1.36\text{mm}$ ; (b).  $L_1=20\text{mm}, L_2=20\text{mm}, \Delta x_{LA}=0.74\text{mm}$ ; and (c).  $L_1=40\text{mm}, L_2=0\text{mm}, \Delta x_{LA}=0.01\text{mm}$ . (1). the object; (2). Conventional imaging; (3)-(4). were images reconstructed by the second-order correlation between two paths when the test detector was a bucket detector, and a CCD camera with the axial resolution  $6.45 \times 6.45\mu\text{m}$ , respectively.

reconstructed by the second-order correlation of two light fields in scattering media. However, if the object is fixed in the middle of the scattering media, the quality of the image is the worst.

In the experiments, we prepare a suspension liquid composed by emulsion polymerization particles with particle diameter  $D=3.26\mu\text{m}$  and the solution *NaCl* with density  $\rho=1.19\text{ g/cm}^3$ . The vessel used to put the suspension liquid is designed as  $40\text{mm} \times 10\text{mm} \times 20\text{mm}$ . We take  $\lambda=650\text{nm}$ ,  $f_1=400.0\text{mm}$ ,  $f=150.0\text{mm}$ ,  $f_2=250.0\text{mm}$ ,  $z=211.0\text{mm}$ ,  $z_1=300.0\text{mm}$ ,  $z_2 + L_2=390.0\text{mm}$ ,  $z_3=243.8\text{mm}$ . The average sizes of the speckles on the CCD camera plane are  $40.6\mu\text{m}$ . When the light goes through the scattering media with thickness  $L_1 + L_2=40\text{mm}$ ,  $|\frac{\partial}{\partial x}|^2 \approx 694$ ,  $\Delta x_{LA} \approx 1.36\text{mm}$ , the scattering coefficient of the medium  $\mu_s \approx 1.64/\text{cm}$ . The minimum characteristic scale of the object (“zhong” ring) is  $60\mu\text{m}$  and the diameter of the ring is  $1.6\text{mm}$ .

Fig. 2(I) represents the point scattering functions when the thermal light goes through different mediums. The Gaussian envelop will become wider because of multiple scattering. For conventional imaging, as shown in Fig. 2(II)(2), the quality of images will reduce as the increase of the scattering thickness  $L_2$ . Oppositely, when the test detector is a bucket detector, the quality of the images reconstructed by the second-order correlation between two paths will decay as the scattering thickness

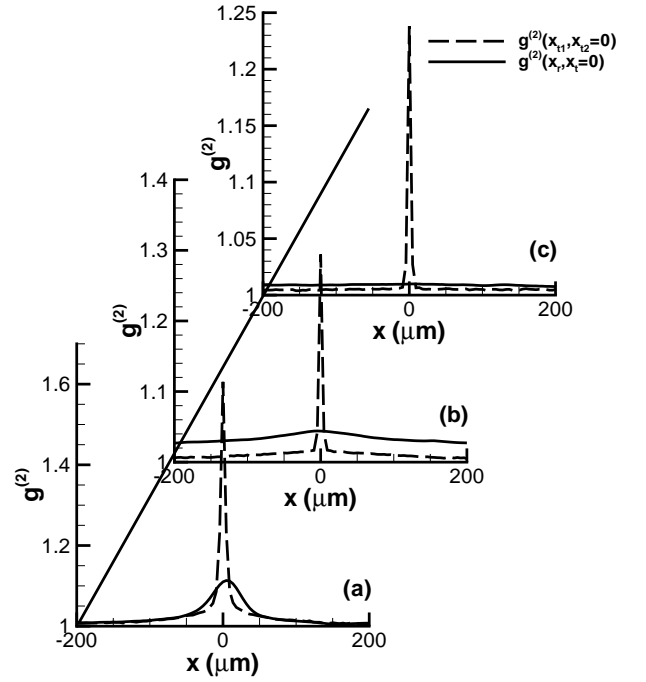


FIG. 3: Effect of multiple scattering between the source and the object plane on  $g^{(2)}(x_{t1}, x_{t2} = 0)$  and  $g^{(2)}(x_r, x_t = 0)$  for different scattering thickness  $L_1$  and  $L_2=0$  without the object. (a).  $L_1=10\text{mm}$ ; (b).  $L_1=20\text{mm}$ ; (c).  $L_1=40\text{mm}$ .

$L_1$  is increased [Fig. 2(II)(3)]. However, as shown in Fig. 2(II)(4-c), if the test detector is a CCD camera with high axial resolution, we can also obtain images with high quality via the second-order correlation of the two light fields when there is only strong multiple scattering between the object plane and the source. In addition, if the object is fixed in the middle of the scattering media, the visibility of the image will reduce, but the resolution doesn’t decay [Fig. 2(II)(4-b)].

The visibility of the images reconstructed by the second-order correlation of two light fields can be explained by normalized second-order correlation function [13]

$$g^{(2)}(x_1, x_2 = 0) = 1 + \frac{\Delta G^{(2,2)}(x_1, x_2 = 0)}{\langle I(x_1) \rangle \langle I(x_2 = 0) \rangle}. \quad (14)$$

where  $g^{(2)}(x_1, x_2 = 0)$  denotes the second-order cross correlation degree between two spatial positions  $x_2=0$  and  $x_1$ . For the thermal light field,  $g^{(2)}(x_{t1}, x_{t2} = 0)$  reveals the fluctuation of the light field, whereas  $g^{(2)}(x_r, x_t = 0)$  describes the cross correlation between two paths. As shown in Fig. 3, both the maximum values of the second-order correlation degree  $g^{(2)}(x_{t1} = 0, x_{t2} = 0)$  and  $g^{(2)}(x_r = 0, x_t = 0)$  decrease sharply as the scattering thickness  $L_1$  is increased, so the visibility of images will reduce (see Fig. 2(II)(3)). However, even  $g^{(2)}(x_r = 0, x_t = 0)$  is lower than 1.05, an image with high quality can still be reconstructed when both the de-

tectors in two paths are CCD cameras with high axial resolution (see Fig. 2(II)(4)).

Because multiple scattering between the source and the object plane destroys the cross-correlation between the two paths, thus the visibility of the image and  $g^{(2)}(x_r = 0, x_t = 0)$  will be degraded as the increase of multiple scattering. Higher  $g^{(2)}(x_r = 0, x_t = 0)$  and larger transverse coherent width on the object plane can both enhance the visibility of the image in scattering media reconstructed by the second-order correlation between the test and reference paths [27, 28].

In addition, by the results described by Eq. (12) and represented in Figs. 2-3, when the both detectors in two paths are CCD cameras with high axial resolution, the quality of images obtained by the second-order correlation of two light fields is also determined by the quality of images registered by the CCD camera  $D_t$ . Thus, almost all existing conventional imaging schemes in scattering media can be applied in the test path to further improve the quality of the correlation imaging system. When  $L_1 \ll L_2$ , the quality of the image reconstructed by the second-order correlation of the two light fields is mainly determined by the mechanism of “ghost” imaging. Because of the separation of detection and imaging for “ghost” imaging, the test detector is only used to collect the radiation of the thermal light propagating through the object, while imaging system is located in the reference path. Because there is no multiple scattering in the reference path, the quality of the image isn’t

influenced. If  $L_1 \gg L_2$ , the quality of the reconstructed image mainly depends on the conventional imaging system in the test path. Because the scattering between the object and the CCD camera  $D_t$  is weak, thus the image with good quality can also be obtained. Generally speaking, by the second-order correlation of the two light fields, we can always obtain an image with much better quality than the image achieved only with conventional first-order correlation optical imaging methods in scattering media. Entangled source and other nonclassical light source with higher  $g^{(2)}(x_{t1} = 0, x_{t2} = 0)$  may be applied to further improve the quality of the image obtained by the second-order correlation imaging system in scattering media [29, 30, 31].

In conclusion, imaging via the second-order correlation of two light fields provides a brand-new route for imaging in scattering media. We demonstrate for the first time that we can always obtain an image with much better quality reconstructed by the second-order correlation imaging method than the image achieved by conventional first-order correlation imaging methods in scattering media. This will be very useful to imaging, test and diagnosis of biological tissues with infrared and near infrared light.

The work was partly supported by the Hi-Tech Research and Development Program of China under Grant Project No. 2006AA12Z115, and Shanghai Fundamental Research Project under Grant Project No. 06JC14069.

- 
- [1] T. S. McKechnie, J. Opt. Soc. Am. A, **8**,2 (1991).  
 [2] Raine D. A. , and Brenizer J. S. Materials evaluation, **55**, 1174 (1997).  
 [3] K. P. Maher, J. F. Malone, and Brain Chance, Contemporary Physics, **38**, 131 (1997).  
 [4] Lihong V. Wang and Hsin-i Wu, Biomedical optics: principle and imaging (Wiley-interscience), (2007).  
 [5] A. P. Gibson, J. C. Hebden and S. R. Arridge, Phys. Med. Biol. **50** R1-R43 (2005).  
 [6] A. Yodh, and B. Chance, Phys. Today, **48**, 34 (1995).  
 [7] S. R. Arridge, Topical Review, R41-93 (1999).  
 [8] H. F. Zhang, K. Maslov, G. Stoica, and L.-H. Wang, Nature Biotechnology **13**, 848C851 (2006).  
 [9] E. L. Hsiung, J. R. Taylor, and V. P. Gaporation, Opt. Exp. **12**, 22 (2004).  
 [10] M. Nieto-Vesperinas, J. Opt. Soc. Am. A, **5**, 360 (1988).  
 [11] B. R. Holstein, Topics in advanced quantum mechanics, P50-54 (1992).  
 [12] A. Gatti, E. Brambilla, and L. A. Lugiato, 2008, Quantum imaging, (E.Wolf, Progress in Optics 51), Chap. 5.  
 [13] R. J. Glauber, Phys. Rev. **130**, 2529 (1963).  
 [14] M. D. Angelo, and Y. H. Shih, Laser. Phys. Lett. **2**, 12. 567-596 (2005).  
 [15] T. B. Pittman, Y. H. Shih, D. V. Strelakov, and A. V. Sergienko, Phys. Rev. A. **52**. R3429 (1995).  
 [16] A. Valencia, G. Scarcelli, M. D’Angelo, and Y. Shih, Phys. Rev. Lett. **94**. 063601 (2005).  
 [17] J. Cheng and S. Han, Phys. Rev. Lett. **92**. 093903 (2004).  
 [18] A. Gatti, E. Brambilla, M. Bache, and L. A. Lugiato, Phys. Rev. Lett. **93**. 093602 (2004).  
 [19] A. Gatti, E. Brambilla, and L. A. Lugiato, Phys. Rev. Lett. **90**. 133603 (2003).  
 [20] R. S. Bennink, S. J. Bentley, R. W. Boyd and J. C. Howell, Phys. Rev. Lett. **92**. 033601 (2004).  
 [21] D. Zhang, Y. Zhai, and L. Wu, Opt. Lett. **30**, 18 (2005).  
 [22] M. Zhang, Q. Wei, X. Shen, Y. Liu, H. Liu, J. Cheng, and S. Han, Phys. Rev. A. **75**, 021803(R) (2007).  
 [23] W. Martienssen, E. Spiller, Am. J. Phys. **32**, 919, (1964).  
 [24] H. Liu, J. Cheng, S. Han, Opt. Commun. **273**, 50 (2007).  
 [25] R. Hassanein, E. Lehmann, and P. Vontobel, Nucl. Ins. Meth. Phys. Res. A. **542**, 353 (2005).  
 [26] P. N. Segrè and P. N. Pusey, Phys. Rev. Lett. **77**, 771 (1996).  
 [27] Shen Xia, Bai Yan-Feng, Qin Tao, and Han Shen-Sheng, Chin. Phys. Lett. **25**, 11 (2007).  
 [28] A. Gatti, M. Bache, D. Magatti, E. Brambilla, F. Ferri, and L. A. Lugiato, J. Mod. Opt. **53**, 739 (2006).  
 [29] K. W. Chan, and J. H. Eberly, arXiv. quantum-ph/0404093v2 (2004).  
 [30] D. F. Walls, Nature (London), **306**, 10 (1983).  
 [31] L.-G. Wang, S.-Y. Zhu, arXiv. Physics. optics/0806.1784v1 (2008).